TÜBİTAK

Turkish Journal of Chemistry

http://journals.tubitak.gov.tr/chem/

Research Article

Turk J Chem
(2016) 40: 38 – 53

doi:10.3906/kim-1502-11

Synthesis and photochromism of new asymmetrical diarylethenes with a variable heteroaryl ring and a quinoline unit

Hongyan XU, Renjie WANG, Congbin FAN, Gang LIU, Shouzhi PU*
Jiangxi Key Laboratory of Organic Chemistry, Jiangxi Science and Technology Normal University, Nanchang, P.R. China

Received: 02.02.2015 • **Accepted/Published Online:** 05.05.2015 • **Final Version:** 05.01.2016

Abstract: Three new asymmetrical photochromic diarylethenes containing a variable heteroaryl ring and a quinoline unit were synthesized and their structures were determined by single-crystal X-ray diffraction analysis. Their properties, including photochromism, acidichromism, and fluorescence, were investigated systematically. For these diarylethenes, the one with an indole moiety had the largest absorption maximum, cyclization quantum yield, photoconversion ratio, emission peak, and fluorescent modulation efficiency. In addition, these diarylethenes exhibited an evident dual switching behavior induced by the stimulation of acid/base and UV/Vis. Addition of trifluoroacetic acid to solution of the diarylethenes produced protonated derivatives with notable changes in their absorption spectra. These results indicated that the effect of the heteroaryl rings played a very important role during the process of photoisomerization for these diarylethene derivatives.

Key words: Diarylethene, photochromism, quinoline moiety, crystal structure, acidichromism, fluorescence

1. Introduction

Organic photochromic materials have received considerable attention because of their potential for photonic applications such as optical storage materials, photoswitches, and organic semiconductor devices.[1–6] So far, various types of photochromic compounds have been developed in an attempt to satisfy the requirements of optoelectronic devices. Among these compounds, diarylethenes are one of the most promising candidates for practical applications because of their remarkable fatigue resistance, excellent thermal stability, and rapid response to the stimulation of light and chemicals.[7–9]

In the past several decades, the design and synthesis of novel diarylethenes with different heteroaryl rings have become an active area. Among the diarylethenes hitherto reported, most of the heteroaryl rings have been thiophene or benzothiophene rings[10–17] with just a few reports concerning other heteroaryl moieties, such as furan,[18] pyrrole,[19] indole,[20] benzofuran,[21] indene,[22] and pyrazole.[23] In general, the nature of the heteroaryl rings can effectively influence the photochromic reactivities of diarylethenes during the process of cyclization and cycloreversion reactions induced by photoirradiation. For example, diarylethenes with five-membered heteroaryl rings showed remarkable thermal stability and excellent fatigue resistance, whereas diarylethenes with a six-membered heteroaryl ring were thermally unstable.[24] Benzothiophene and benzofuran are fascinating aryl rings because of their low aromatic stabilization energies.[25,26] As another interesting aryl unit, indole can dramatically enhance the fluorescence modulation efficiency of the diarylethenes.[20] The three heteroaryl rings have similar

*Correspondence: pushouzhi@tsinghua.org.cn

chemical structures with different electron cloud distributions, so that they are representative candidates to study the heteroaryl effect on the photochromic properties of diarylethenes. In this work, we designed and synthesized three novel asymmetrical diarylethenes, which have a benzothiophene (**1o**), benzofuran (**2o**), and indole moiety (**3o**), respectively (Scheme 1). Their single structures and properties were also systematically investigated.

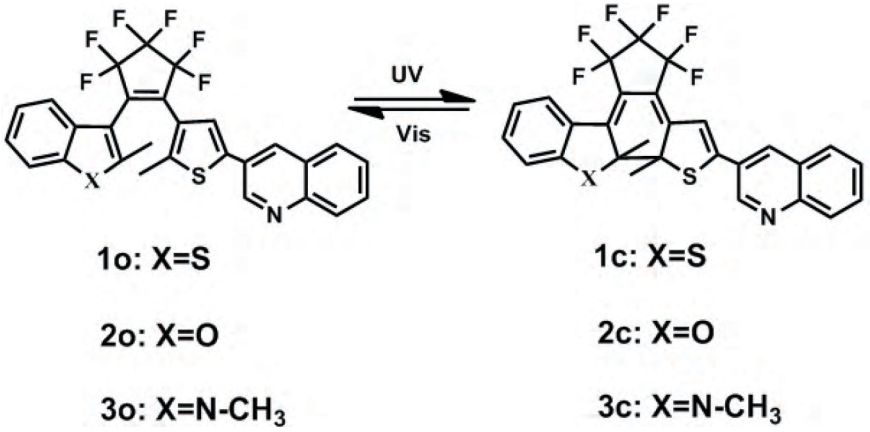

Scheme 1. Photochromism of diarylethenes **1** − **3**.

2. Results and discussion

2.1. Photochromism

The photochromic behaviors of diarylethenes **1** − **3** induced by photoirradiation were measured in acetonitrile ($C = 2.0 \times 10^{-5}$ mol L^{-1}) and PMMA films (10%, w/w) at room temperature. The absorption spectral change of **1** and color changes of **1**–**3** by photoirradiation are shown in Figures 1A–1C. Upon irradiation with 297 nm light, the colorless acetonitrile solution of **1o** turned purple and a new visible absorption band centered at 551 nm emerged (Figure 1A). The original peak formed by $\pi \rightarrow \pi^*$ transition at 264 nm decreased,[27] indicating that the cyclization reaction occurred and the closed-ring isomer **1c** was generated. Alternatively, the purple solution of **1c** could be bleached entirely upon irradiation with visible light ($\lambda pp. > 500$ nm). In the photostationary state, a clear isosbestic point was observed at 352 nm, which supported the reversible two-component photochromic reaction scheme.[28] Diarylethenes **2** and **3** showed similar photochromism in acetonitrile (Figures S1A and S1B, Supplementary information (SI); on the journal's website). Upon irradiation with 297 nm light, the colorless solution of **2o** turned magenta and that of **3o** turned green due to the formation of the closed-ring isomers **2c** and **3c** (Figure 1C), for which the absorption maxima were observed at 537 and 615 nm, respectively. Both the colored solutions of **2c** and **3c** could be bleached completely upon irradiation with appropriate visible light ($\lambda pp. > 500$ nm). When reached at the photostationary state, the isosbestic points of **2** and **3** were observed at 353 nm and 339 nm in acetonitrile, respectively.

The photoconversion ratios from open-ring to closed-ring isomers of **1**–**3** were analyzed by ^{1}H NMR method in the photostationary state. It could be easily calculated that the photoconversion ratios of diarylethenes **1**–**3** are 30% for **1**, 42% for **2**, and 68% for **3** (Figure 2). In PMMA amorphous films, diarylethenes **1**–**3** also showed similar photochromism as observed in solution. Upon irradiation with 297 nm light, the colorless films containing **1**–**3** turned purple, magenta, and green, respectively, due to the formation of the closed-ring forms **1c**–**3c**. The absorption maxima of **1c**–**3c** in PMMA films were observed at 556 nm, 537 nm, and 615 nm,

respectively (Figure 1B, Figures S2A and S2B, SI). Reversely, the colored films could be bleached by irradiation with appropriate visible light ($\lambda pp. > 500$ nm).

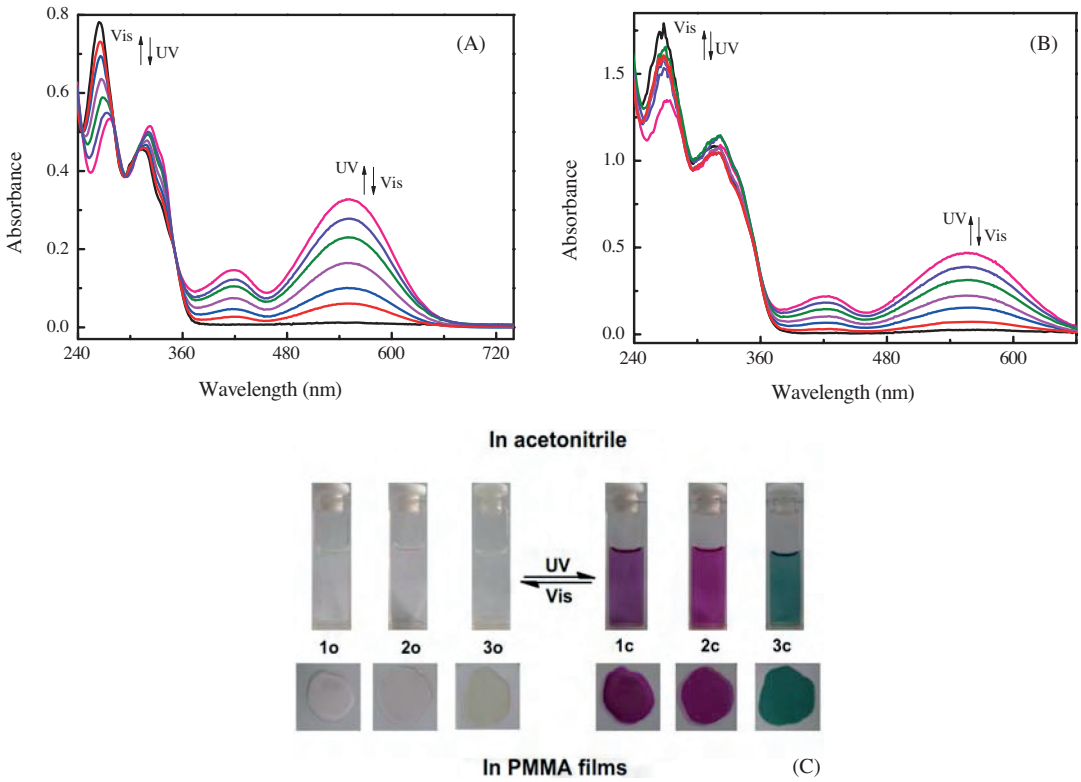

Figure 1. Absorption spectra of **1** and the color changes of **1**–**3** upon alternating irradiation with UV and visible light in solution and solid media: (A) spectral changes of **1** in acetonitrile (2.0×10^{-5} mol L^{-1}), (B) spectral changes of **1** in a PMMA film (10%, w/w), (C) color changes of **1**–**3**.

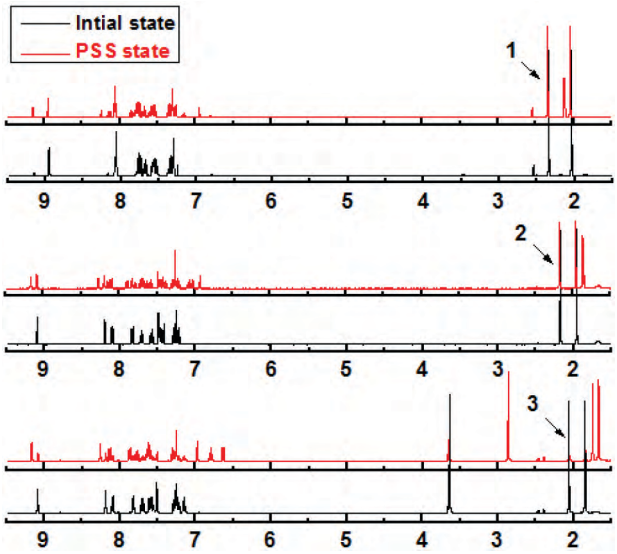

Figure 2. The ^{1}H NMR spectrum changes of diarylethenes **1** − **3** in the photostationary state (PSS) in $CDCl_3$.

The photochromic properties of diarylethenes **1**–**3** are summarized in Table 1. It was noted that different heteroaryl rings had a significant effect on the photochromic features of these diarylethene derivatives. Although the absorption maxima of the open-ring isomers **1o**–**3o** did not evidently change, the absorption maxima of the closed-isomers **1c**–**3c** and quantum yield exhibited remarkable changes with the variable heterocyclic moieties. Among the three analogs, the diarylethene with an indoly moiety (**3**) has the biggest visible absorption peak and cyclization quantum, but the lowest absorption value. When the indole ring was replaced with a benzothiophene (**1**) or benzofuran moiety (**2**), the absorption maximum of the closed-ring isomers and the cyclization quantum yield decreased evidently. Compared with the benzofuran moiety (**2**), the absorption maximum of **3c** showed a remarkably bathochromic shift with 77 nm. The result indicated that the indole ring could effectively shift the absorption maximum to a long wavelength. Furthermore, the molar absorption coefficients of open-ring isomers **1o**–**3o** increased in the order indolyl < benzofuranyl < benzothienyl, and the absorption value of closed-ring isomers **1c**–**3c** increased in the order indolyl < benzothienyl < benzofuranyl. For diarylethenes **1**–**3**, the cyclization quantum yield and photoconversion ratio of **3** are the largest and those of **1** are the smallest. The results indicated that variable heterocyclic moieties played a vital role during the process of photoisomerization of these diarylethenes.

Table 1. Absorption characteristics and photochromic reactivity of diarylethenes $\mathbf{1-3}$ in acetonitrile (2.0×10^{-5} mol L^{-1}) and in PMMA films (10%, w/w).

Compd.	$\lambda_{o,max}$/nm[a] (ε/L mol^{-1} cm^{-1})		$\lambda_{c,max}$/nm[b] (Absorbance value)		Φ[c]		*PR*/%[d]
	Acetonitrile	PMMA film	Acetonitrile	PMMA film	Φ_{o-c}	Φ_{c-o}	
1	264 (3.91×10^4)	268	551 (0.328)	556	0.20	0.02	30
2	264 (3.51×10^4)	264	537 (0.368)	538	0.30	0.04	42
3	265 (3.03×10^4)	264	615 (0.193)	615	0.37	0.04	68

[a]Absorption maxima of open-ring isomers.
[b]Absorption maxima of closed-ring isomers.
[c]Quantum yields of open-ring (Φ_{o-c}) and closed-ring isomers (Φ_{c-o}).
[d]Photoconversion ratios in the photostationary state.

The fatigue resistances of diarylethenes **1**–**3** were examined in both acetonitrile (2.0×10^{-5} mol L^{-1}) and PMMA films (10%, w/w) by alternating irradiating with 297 nm UV and visible light ($\lambda pp. > 500$ nm) at room temperature. The result is depicted in Figures 3A and 3B. In acetonitrile, the coloration and decoloration cycles of **1**–**3** could repeat 100 cycles with only ca. 6% degradation of **1c**, 8% degradation of **2c**, and 12% degradation of **3c** (Figure 3A). The degradation may be ascribed to the formation of epoxide.[29] In PMMA films, the diarylethenes exhibited much stronger fatigue resistance than in the solution due to the effective suppression of the oxygen diffusion. After 200 repeating cycles, they still showed favorable photochromism with only ca. 6% degradation of **1c**, 12% degradation of **2c**, and 15% degradation of **3c** (Figure 3B). As a result, the fatigue resistance of the three diarylethenes was significantly enhanced in the order benzothienyl > benzofuranyl > indolyl in both solution and PMMA films, indicating that the diarylethene with a benzothiophene and a thiophene (**1**) had the strongest fatigue resistance in both solution and solid medium, which was attributed to its lower reactivity to singlet oxygen and the prohibition of formation of the six-membered ring byproduct from the benzothiophene moiety.

Single crystals of **1o**–**3o** were obtained via slow evaporation of ethyl acetate/hexane cosolvent system and subjected to X-ray diffraction analysis. Their ORTEP drawings and photochromic processes in the crystalline phase are shown in Figures 4A–4E, and the X-ray crystallographic analysis data are listed in Table 2. For

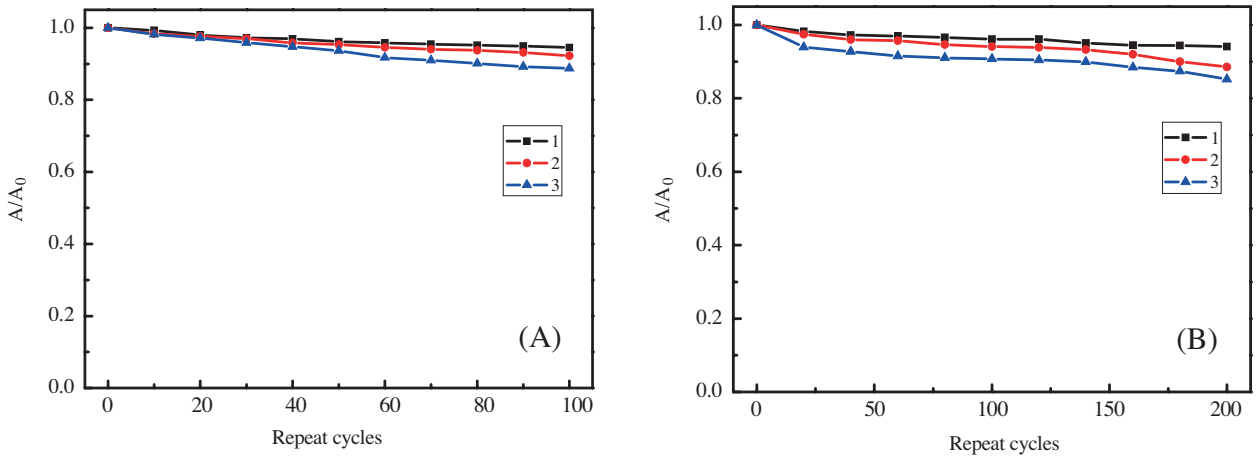

Figure 3. Fatigue resistance of diarylethenes **1** − **3** in air atmosphere at room temperature: (A) in acetonitrile, (B) in PMMA films. Initial absorbance of the sample was fixed to 1.0.

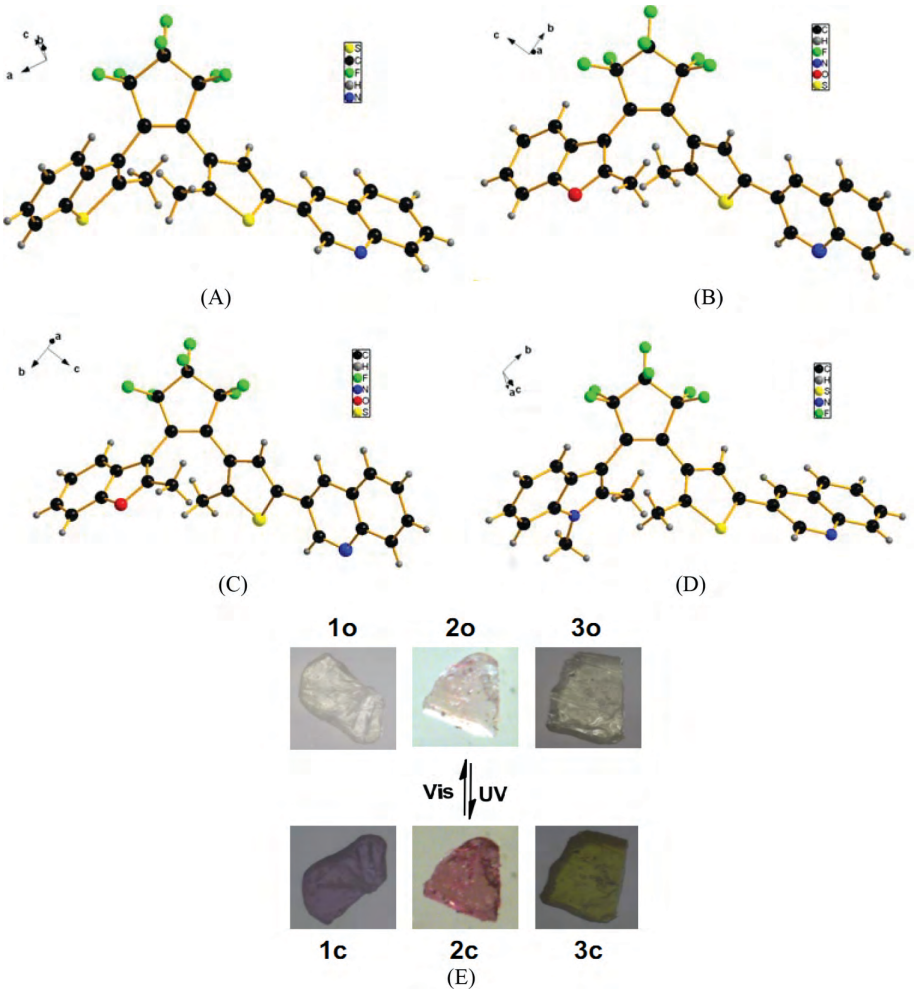

Figure 4. ORTEP drawings of crystals **1o**–**3o** and their photochromism in the crystalline phase: (A) ORTEP drawing of **1o**, (B) ORTEP drawing of **2o-I**, (C) ORTEP drawing of **2o-II**, (D) ORTEP drawing of **3o**, (E) photos demonstrating their photochromic processes in the crystalline phase.

the crystal of **1o**, the crystal system and space group were orthorhombic and Pbca (Figure 4A), and the unit cell dimension was 1.493 g cm^{-3}. The two methyl groups were located on different sides of the double bond and trans-direction of the benzothiophene and thiophene planes. The dihedral angles between the central cyclopentene ring and the two thiophene rings are 68.4° for S1/C4/C5–C7/C8 and 57.9° for S2/C16–C19. The dihedral angle between the thiophene ring and the adjacent quinoline ring is 8.1°. The intramolecular distance between the two reactive carbon atoms (C8...C16) is 4.135 Å. In the single crystal of **2o**, there were two asymmetrical and independent molecules (molecule **2o-I** and molecule **2o-II**) and both of them adopted an antiparallel conformation in the asymmetric unit (Figures 4B and 4C). The distances between the photoactive carbons (C8...C16 and C36...C44) in each molecule were 3.549 and 3.581 Å, respectively. The crystal system and space group of **3o** were triclinic and P-1 (Figure 4D), which may be attributed to the coordinating effects of the methylindole moiety. It packs in the photoactive antiparallel conformation in the crystalline phase and the distance between the two reactive carbon atoms (C13...C28) is 3.598 Å. Their corresponding dihedral angles and the distances of **1o**–**3o** are shown in Table 3. Based on the empirical rule that the molecule can be expected to undergo the photocyclization reaction if the molecule is fixed in an *anti*-parallel mode and the distance between reacting carbon atoms on the aryl rings is less than 4.2 Å,[30,31] the crystals of **1o**–**3o** could be expected to display photochromism in the crystalline phase. As expected, the three diarylethenes exhibited photochromism by photoirradiation in the crystalline phase (Figure 4E).

Table 2. Crystal data for diarylethenes **1o** − **3o**.

	1o	**2o**	**3o**
Formula	$C_{28}H_{17}F_6NS_2$	$C_{56}H_{34}F_{12}N_2O_2S_2$	$C_{29}H_{20}F_6N_2S$
Formula weight	545.56	1058.97	542.53
Temperature	296(2)	296(2)	296(2)
Crystal system	Orthorhombic	Orthorhombic	Triclinic
Space group	Pbca	Pna2(1)	P-1
Unit cell dimensions a (Å)	11.2971(12)	12.4154(3)	8.6376(10)
b(Å)	18.011(2)	9.7336(2)	11.4812(13)
c(Å)	23.853(3)	39.2147(9)	13.9472(16)
α (^{o})	90	90	107.8790(10)
β (^{o})	90	90	96.7420(10)
γ (^{o})	90	90	94.2130(10)
Volume (Å^3)	4853.3(9)	4738.96(19)	1298.4(3)
Z	8	4	2
Reflections collected	5551	10054	5641
Reflections observed	4409	8117	4615
Number of parameters	334	671	346
Density (calcd.) (g/cm^3)	1.493	1.484	1.388
Goodness-of-fit on F^2	1.044	1.096	1.636
Final R_1 [I > 2s(I)]	0.0535	0.0529	0.0958
wR_2 [I > 2s(I)]	0.1498	0.1464	0.3390
R_1 (all data)	0.0687	0.0667	0.1091
wR_2 (all data)	0.1664	0.1563	0.3642

The packing diagrams of **1o**–**3o** in the unit cell are shown in Figures 5A–5C. Neighboring molecules are *anti*-parallel and crisscross each other in the cell. For the crystal of **1o** (Figure 5A), molecules are arranged by the intermolecular C–H...F hydrogen bonds with an average H...F distance of 2.50 Å and C–H...F angle of 130°, and intermolecular hydrogen bonds C–H···S with an average H...S distance of 2.65 Å and C–H...S angle of 110° (Table 4). In the crystal of **2o** (Figure 5B), there were more intermolecular hydrogen bonds (C–H...S and C–H...F) to connect the molecules with each other. Two molecules are arranged in a head-to-tail style to afford a dimeric moiety through the intermolecular C–H...S hydrogen bonds with H...S distance of 2.56-2.58 Å and C–H...S angle of 112°, and C–H...F hydrogen bonds with H...F distance of 2.44–2.54 Å and C–H...F angle of 111–135°. Similarly, for the crystal of **3o** (Figure 5C), molecules are arranged through intermolecular C–H...F hydrogen bonds with an average H...F distance of 2.39–2.51 Å and C–H...F angle of 118–121°, and intermolecular hydrogen bonds C–H···S with an average H...S distance of 2.80 Å and C–H...S angle of 107°. These molecular interactions together with hydrogen bonding enhanced the stability of the framework.

Table 3. Distances between the reacting carbon atoms d (Å) and dihedral angles θ (°) of diarylethenes **1o**−**3o**.

Compd	d(Å)		θ (°)[a]		
			θ_1	θ_2	θ_3
1o	C8...C16	4.135	68.4	57.9	8.1
2o-I	C8...C16	3.549	46.4	44.5	5.6
2o-II	C36...C44	3.581	48.1	44.76	6.6
3o	C13...C28	3.598	50.1	41.7	28.6

[a] θ_1, Dihedral angle between the hexafluorocyclopentene ring and the adjacent heteroaryl ring; θ_2, dihedral angle between the hexafluorocyclopentene ring and the thiophene ring; θ_3, dihedral angle between the thiophene ring and the quinoline ring.

Table 4. Hydrogen bond length (Å) and bond angle (°) of diarylethene **1o**−**3o**.

Crystal	D–H...A	D–H	H...A	D...A	D–H...A
1o	C(9)–H(9A)...F(5)	0.96	2.50	3.204(4)	130
	C(24)–H(24A)...S(2)	0.93	2.65	3.095(3)	110
2o	C(4)–H(4)...F(2)	0.93	2.44	3.164(5)	135
	C(17)–H(17C)...F(5)	0.96	2.46	3.163(7)	130
	C(28)–H(28)...S(1)	0.93	2.56	3.034(4)	112
	C(32)–H(32)...F(11)	0.93	2.49	3.197(4)	133
	C(45)–H(45C)...F(8)	0.96	2.52	3.202(6)	128
	C(46)–H(46)...F(8)	0.93	2.54	3.002(6)	111
	C(56)–H(56)...S(2)	0.93	2.58	3.047(4)	112
3o	C(9)–H(9)...S(1)	0.93	2.80	3.190(4)	107
	C(11)–H(11)...F(6)	0.93	2.51	3.058(5)	118
	C(22)–H(22)...F(1)	0.93	2.39	2.974(7)	121

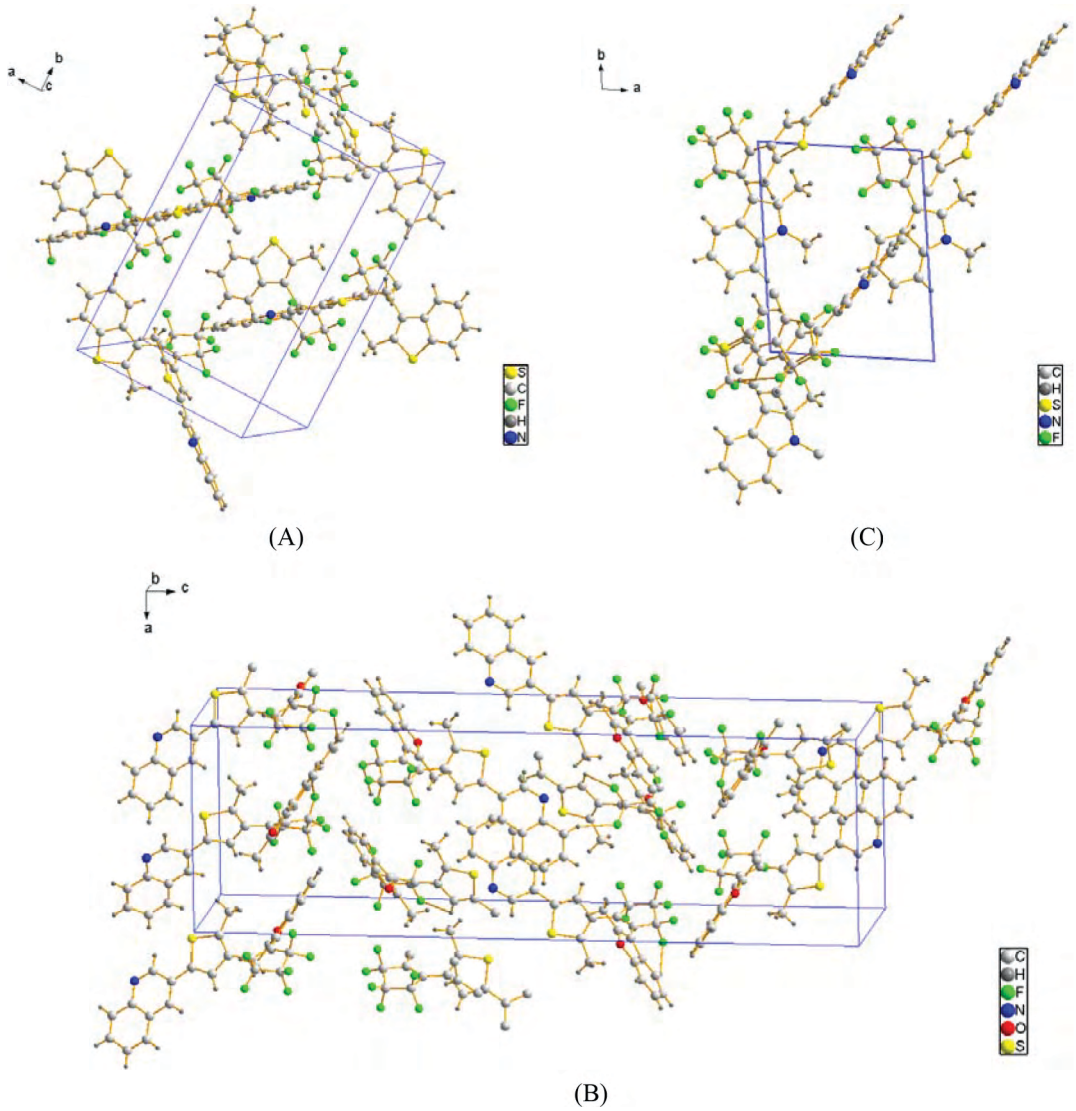

Figure 5. Packing diagrams of **1o**–**3o** along *a* direction: (A) **1o**, (B) **2o**, (C) **3o**.

2.2. Acidichromism

The nitrogen atom of the quinoline ring is basic and can participate in acid–base reactions. A diarylethene containing a quinoline unit can thus be tuned with proton. The absorption spectral change of **1** induced by proton and light is shown in Figure 6A. Gradual addition of trifluoroacetic acid (TFA) to **1o** in acetonitrile redshifted the absorption maximum from 276 nm to 281 nm due to the formation of protonated **1o′**, which could be converted back into **1o** by neutralization with triethylamine (TEA). Upon irradiation with UV light, the colorless solution of **1o′** turned purple, indicating the formation of *N*-protonated ring-closed isomer **1c′**. Its absorption maximum was observed at 558 nm. Alternatively, an interconversion between diarylethenes **1c** and **1c′** could be conducted by stimulation with acid/base. The bathochromic shift of the absorption spectrum of **1c′** was possibly due to the lowered excited state energy levels of the protonated form. Similar phenomena were observed for diarylethenes **2** and **3**. Upon irradiation with UV light, the absorption maxima of **2c′** and **3c′** exhibited evident redshifts with the value of 5 nm and 23 nm (Figures 6B and 6C), respectively.

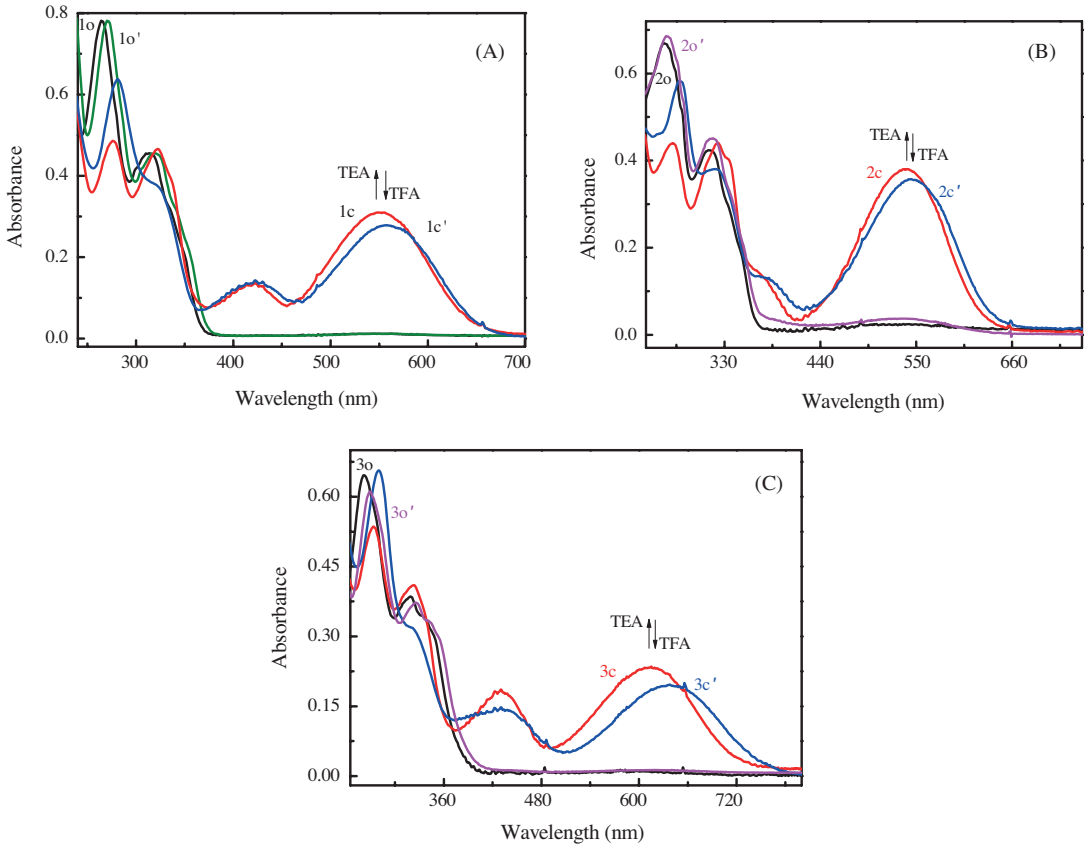

Figure 6. The absorption spectral changes of diarylethenes **1**–**3** by the stimulation of TFA and TEA in acetonitrile: (A) **1**, (B) **2**, (C) **3**.

2.3. Fluorescence

The fluorescence behaviors of **1o**–**3o** were studied in both acetonitrile (2.0×10^{-5} mol L^{-1}) and PMMA films (10%, w/w) at room temperature, and the results are shown in Figures 7A and 7B and Table 5. In acetonitrile, the emission peaks of **1o**–**3o** were observed at 419 nm (λ_{ex}, 320 nm), 385 nm (λ_{ex}, 346 nm), and 478 nm (λ_{ex}, 354 nm), respectively (Figure 7A). In PMMA films, the emission peaks were observed at 418 nm (λ_{ex}, 320 nm) for **1o**, 420 nm (λ_{ex}, 283 nm) for **2o**, and 425 nm (λ_{ex}, 370 nm) for **3o** (Figure 7B). Compared to those in acetonitrile, the emission peak of **2** in a PMMA film exhibited a bathochromic shift with the value of 35 nm, while that of **3** exhibited an obvious hypsochromic shift with the value of 53 nm. By using anthracene as a reference, the fluorescence quantum yields were determined as 0.024 for **1o**, 0.007 for **2o**, and 0.008 for **3o**.

As observed for most reported diarylethenes,[32–36] **1o**–**3o** exhibited evident fluorescence switching properties by photoirradiation. Figures 8A and 8B show the fluorescence changes of **1** by photoirradiation in both acetonitrile and a PMMA film at room temperature. Upon irradiation with 297 nm, the emission intensity of **1** was quenched to ca. 75% in acetonitrile (Figure 8A) and 16% in a PMMA film (Figure 8B) when reached at the photostationary state. Therefore, the fluorescent modulation efficiency of derivative **1** was 25% in acetonitrile and 84% in a PMMA film. Similarly, the fluorescence modulation efficiency values of **2** and **3** were 25% and 69% in acetonitrile, respectively (Figures S3A and S3B, SI). In PMMA films, the fluorescence modulation efficiencies of **2** and **3** were determined to be 82% and 86%, respectively (Figures S4A and S4B, SI). Com-

pared to benzothiophene and benzofuran rings, diarylethene with an indole moiety exhibited greater fluorescent modulation efficiency in both solution and solid media, which may be attributed to its higher photoconversion efficiency in the photostationary state (Table 1). Therefore, the diarylethene with an indole moiety could be potentially suitable for use as an optical memory medium by fluorescence readout method or a fluorescent photoswitch.[37–39]

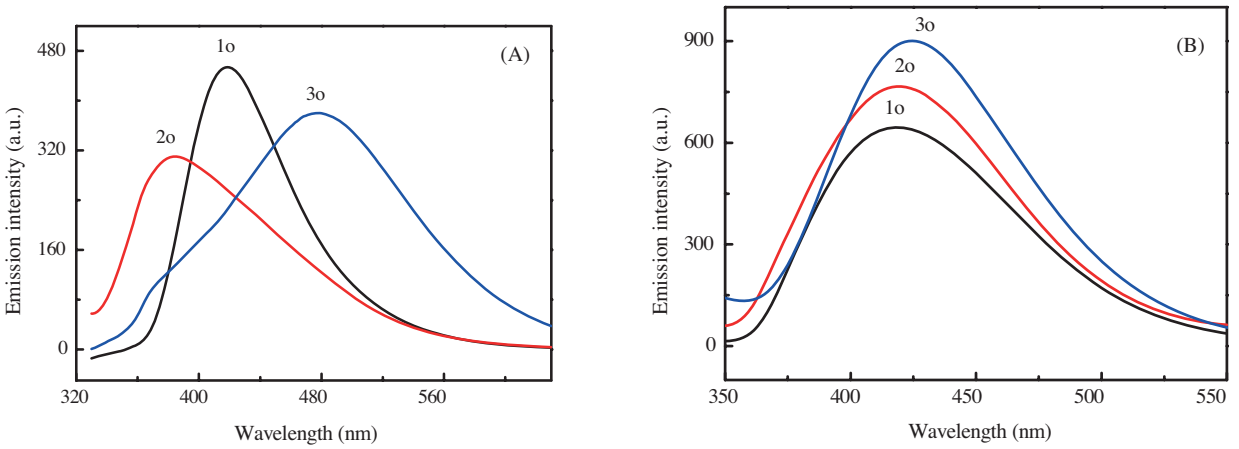

Figure 7. Fluorescence emission spectra of diarylethenes **1**−**3** at room temperature: (A) in acetonitrile (2.0×10^{-5} mol L^{-1}), (B) in PMMA films (10%, w/w).

Table 5. Fluorescence parameters of diarylethenes **1**–**3** in acetonitrile (2.0×10^{-5} mol L^{-1}) and PMMA films (10%, w/w).

	Acetonitrile			PMMA			Φ_f
	λ^a_{em}	I^b_f	η^c (%)	λ^a_{em}	I^b_f	η^c (%)	
1o	419	454	25	418	645	84	0.024
2o	385	310	25	420	766	82	0.007
3o	478	380	69	425	901	86	0.008

[a] Emission peak. [b] Emission intensity. [c] Fluorescence modulation efficiency in the photostationary state.

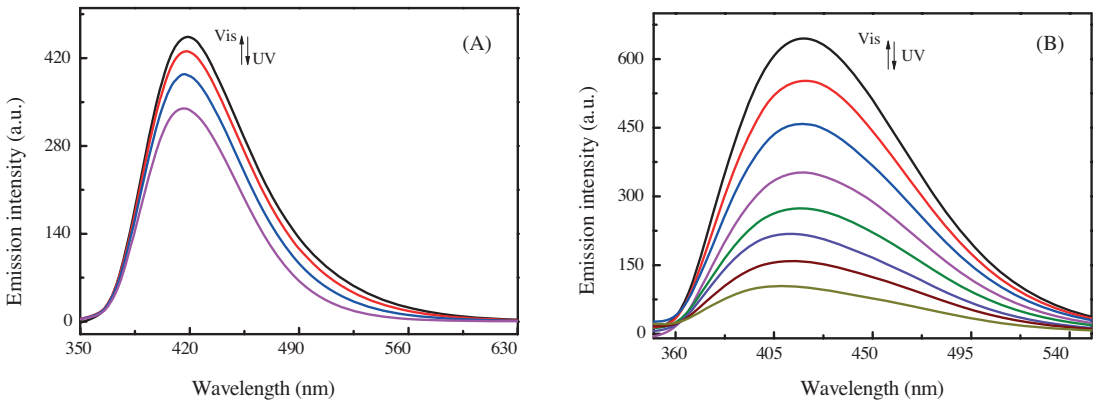

Figure 8. Emission intensity changes of diarylethene **1** by photoirradiation at room temperature: (A) in acetonitrile (2.0×10^{-5} mol L^{-1}), (B) in a PMMA film (10%, w/w).

2.4. Electrochemistry of diarylethenes

The photochromic reaction of diarylethene compounds can be initiated not only by light irradiation but also by an electrochemical.[40,41] In the past decades, the electric properties of diarylethenes have been extensively reported.[42–44] In order to investigate the heteroaryl rings' effect on the electrochemical properties of diarylethenes **1**–**3**, cyclic voltammetry tests were performed under the same experimental conditions at a scanning rate of 50 mV s^{-1}. The electrolyte was acetonitrile (5.0 mL) containing 0.5 mmol tetrabutylammonium tetrafuoroborate ((TBA)BF_4) and 0.2 mmol diarylethene sample. Figure 9 shows the cyclic voltammetry curves of diarylethenes **1**–**3**. The oxidation onsets of **1o**–**3o** were observed at 1.68, 1.60, and 1.55 V, and those of **1c**–**3c** were observed at 1.31, 1.22, and 1.13 V, respectively. Therefore, the difference in oxidation onset between the open-ring and the closed-ring isomers of diarylethenes **1**–**3** was 0.37 V for 1, 0.38 V for 2, and 0.42 V for 3. The result indicated that the oxidation process for the open-ring isomers **1o**–**3o** occurred at higher potentials than in the corresponding closed-ring isomers **1c**–**3c**, indicating that shorter conjugation length leads to larger positive potentials.[45] Among the diarylethenes **1**–**3**, the diarylethene **1** containing benzothienyl showed the biggest oxidation onsets both for the open-ring and the closed-ring isomers. When the benzothienyl group was replaced with benzofuranyl or indolyl ring the oxidation onsets notably decreased. According to the reported method,[46,47] the highest occupied molecular orbitals (HOMO) and the lowest unoccupied molecular orbitals (LUMO) energy levels could be estimated by using the energy level of ferrocene as a reference. Based on the HOMO and LUMO energy levels, the band-gap (Eg) of each compound could be calculated approximately. Their electrochemical characteristics are summarized in Table 6. The data showed that the band-gaps increased in the order **3** < **2** < **1**. The results suggested that the heteroaryl ring has a significant effect on the electrochemical properties of these diarylethenes.

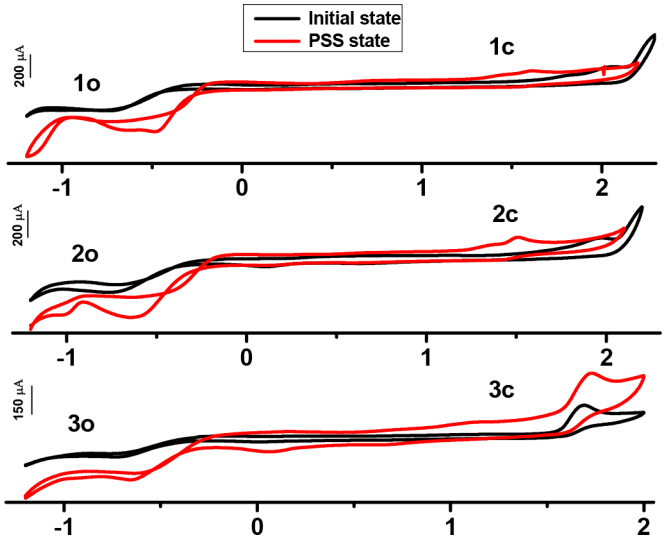

Figure 9. Cyclic voltammetry of diarylethenes **1**–**3** in 0.1 mol/L ((TBA)BF_4) with a scan rate of 50 mV/s.

3. Experimental

3.1. General

The solvents were purified by distillation before use. NMR spectra were recorded on a Bruker AV400 (400 MHz) spectrometer with $CDCl_3$ as the solvent and tetramethylsilane as an internal standard. IR spectra were

recorded on a Bruker Vertex-70 spectrometer. Mass spectra were performed with a LTQ Orbitrap XL mass spectrometer. Melting point was determined by a WRS-1B melting point determination apparatus. Elemental analysis was measured with a PE CHN 2400 analyzer. The absorption spectra were measured using an Agilent 8453 UV/Vis spectrometer. Photo-irradiation was carried out using a SHG-200 UV lamp, CX-21 ultraviolet fluorescence analysis cabinet, and a BMH-250 Visible lamp. Light of appropriate wavelengths was isolated by different light filters. The fluorescent property was measured using a Hitachi F-4600 spectrophotometer, and the breadths of excitation and emission slits were both selected as 5 nm. The X-ray experiment of the single-crystal was performed on a Bruker SMART APEXII CCD diffractometer by using a MULTI scan technique at 294(2) K and Mo Kα radiation. Crystal structures were solved through direct methods and refined through full-matrix least-squares procedures on F^2 in the SHELXTL-97 program. All nonhydrogen atoms were refined anisotropically. Further details of the crystal structure investigation have been deposited with the Cambridge Crystallographic Data Centre as supplementary publication CCDC 1022440 for **1o**, 1022441 for **2o**, and 1022436 for **3o**. Copies of the data can be obtained, free of charge, on application to CCDC, 12 Union Road, Cambridge CB2 1EZ, UK (fax: +44 0 1223 336033 or e-mail: deposit@ccdc.cam.ac.uk).

Table 6. Electrochemical properties of diarylethenes **1**–**3** in acetonitrile.

Compd	Oxidation		Reduction		Band gap
	E_{onset} (V)	IP (eV)	E_{onset} (V)	EA (eV)	E_g
1o	+1.68	–6.48	–0.40	–4.40	2.08
1c	+1.31	–6.11	–0.26	–4.54	1.57
2o	+1.60	–6.40	–0.38	–4.42	1.98
2c	+1.22	–6.02	–0.28	–4.52	1.50
3o	+1.55	–6.35	–0.40	–4.40	1.95
3c	+1.13	–5.93	–0.34	–4.46	1.47

3.2. Synthesis

The synthetic route for diarylethenes **1o**–**3o** is shown in Scheme 2. Suzuki coupling of 3-bromoquinoline and thiophene boronic acid gave the quinolylthiophene **5**. Compound **5** was lithiated and then separately coupled with the monosubstituted **6a**–**c** to give diarylethenes **1o**–**3o**, respectively.[48,49] The structures of **1o**–**3o** were confirmed by elemental analysis, NMR, IR, and crystal structure. The PMMA films of **1o**–**3o** were prepared by dissolving 10 mg of diarylethene sample and 100 mg of polymethylmethacrylate (PMMA) in chloroform (1 mL) with the aid of ultrasound, and then the homogeneous solution was spin-coated on a quartz substrate (20 $\times$ 20 $\times$ 1 mm^3) with a rotating speed at 1500 rpm.

3.2.1. 3-Bromo-2-methyl-5-(3-quinoline)thiophene (5)

Compound **5** was prepared by reacting 3-bromo-2-methyl-5-thienylboronic acid[50] (5.52 g, 25.00 mmol) with 3-bromoquinoline (5.20 g, 25.00 mmol) in the presence of $Pd(PPh_3)_4$ and Na_2CO_3 (6.40 g, 60.00 mmol) in THF (80 mL containing 10% water) for 15 h at 368 K. After the reaction, it was allowed to cool to room temperature. After being extracted with ethyl acetate, the organic layer was dried over $MgSO_4$, filtered, and concentrated. The crude product was purified by column chromatography on silica gel using petroleum ether as eluent to afford 5.40 g of **5** as a pale yellow solid in 71% yield; mp: 405 – 406 K; ^{1}H NMR (400 MHz, $CDCl_3$): δ2.38 (s, 3H), 7.19 (s, 1H), 7.47 (t, 1H, J = 7.4 Hz), 7.60 (t, 1H, J = 8.0 Hz), 7.63 (d, 1H, J = 8.0 Hz), 7.72 (d,

1H, J = 8.0 Hz), pp. 8.07 (s, 1H), pp. 9.01 (s, 1H); ^{13}C NMR (100 MHz, $CDCl_3$, TMS): δ14.9, 110.5, 126.6, 126.9, 127.4, 127.8, 127.9, 129.3, 129.5, 130.9, 135.2, 137.5, 147.3, 147.9; HRMS-ESI (m/z): $[M+H]^+$ Calcd. For ($C_{14}H_{10}BrNS$) 303.9790, found: 303.9781.

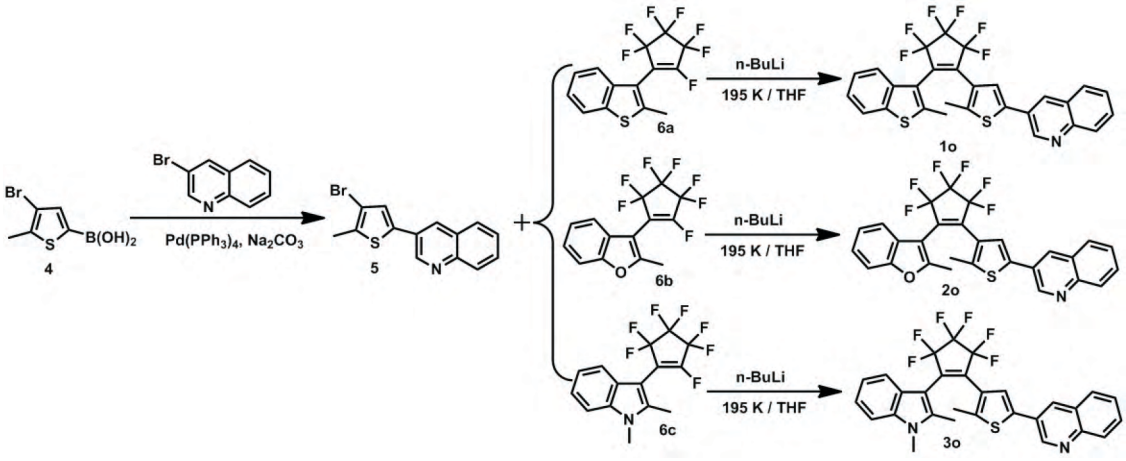

Scheme 2. Synthetic route for diarylethenes **1** − **3**.

3.2.2. 1-(2-Methyl-3-benzothiopheneyl)-2-[2-methyl-5-(3-quinoline)-3-thienyl]perfluorocyclopentene (1o)

To a stirred anhydrous THF (60 mL) of **5** (1.36 g, 3.00 mmol) was slowly added a 2.4 M n-BuLi solution (1.31 ml, 3.15 mmol) at 195 K under an argon atmosphere. After 30 min, THF (10 mL) containing the mixtures of 2-methyl-3-benzothiophene-perfluorocyclopentene (**6a**) (1.02 g, 3.00 mmol) was added and the reaction mixture was stirred for 2 h at this temperature. The reaction was allowed to warm to room temperature and quenched by addition of water. The product was extracted with ethyl acetate. The combined organic layers were dried over anhydrous $MgSO_4$, filtered, and concentrated. The crude product was purified by column chromatography on silica gel using petroleum ether and ethyl acetate (v/v = 15/1) as the eluent to afford 0.16 g of diarylethene **1o** as a faint red solid in 12% yield. Calcd for $C_{28}H_{17}F_6NS_2$ (%): Calcd C, 61.64; H, 3.14; N, 2.57; Found C, 61.60; H, 3.11; N, 2.51; mp: 414–415 K; ^{1}H NMR (400 MHz, $CDCl_3$): δ 2.04 (s, 3H), 2.34 (s, 3H), 7.23 (s, 1H), 7.31–7.37 (m, 2H), 7.53 (d, 1H, J = 8.0 Hz), 7.58 (d, 1H, J = 8.0 Hz), 7.68 (t, 1H, J = 8.0 Hz), 7.76 (t, 2H, J = 8.0 Hz), 8.07 (d, 2H, J = 8.0 Hz), 8.95 (s, 1H); ^{13}C NMR (100 MHz, $CDCl_3$): δ14.9, 120.2,122.0, 122.1, 122.2, 124.0, 124.4, 124.6, 125.0, 125.6, 126.4, 126.7, 127.4, 127.7, 127.8, 129.3, 129.4, 129.6, 131.3, 138.3, 138.4, 142.5, 142.9, 147.4, 147.9; IR (v, KBr, cm^{-1}): 537, 573, 747, 783, 904, 969, 987, 1053, 1103, 1135, 1194, 1271, 1339; HRMS-ESI (m/z): $[M+H]^+$ Calcd. For ($C_{28}H_{18}F_6NS_2$) 546.0779, found: 546.0764.

3.2.3. 1-(2-Methyl-3-benzofuranyl)-2-[2-methyl-5-(3-quinoline)-3-thienyl]perfluorocyclopentene (2o)

Diarylethene **2o** was prepared by a method similar to that used for **1o**. The crude product was purified by column chromatography on silica gel using petroleum ether and ethyl acetate (v/v = 6/1) as eluent to afford 0.33 g of compound **2o** as a reddish solid in 21% yield. Calcd for $C_{28}H_{17}F_6NOS$ (%): Calcd C, 63.51; H, 3.24; N, 2.65. Found C, 63.48; H, 3.22; N, 2.62; mp: 407–408 K; ^{1}H NMR (400 MHz, $CDCl_3$): δ 1.96 (s, 3H), 2.18

(s, 3H), 7.22 (t, 1H, J = 8.0 Hz), 7.29 (t, 1H, J = 8.0 Hz), 7.43–7.48 (m, 2H), 7.50 (s, 1H), 7.58 (t, 1H, J = 8.0 Hz), 7.72 (t, 1H, J = 8.0 Hz), 7.84 (d, 1H, J = 8.0 Hz), 8.11 (d, 1H, J = 8.0 Hz), 8.20 (s, 1H), 9.09 (s, 1H); ^{13}C NMR (100 MHz, $CDCl_3$): δ13.4, 14.8, 105.4, 111.1, 113.6, 113.8, 119.9, 120.0, 120.1, 123.7, 123.8, 124.7, 126.1, 126.2, 126.5, 127.5, 127.8, 127.9, 129.4, 129.7, 131.3, 138.8, 142.6, 147.5, 148.0, 154.2, 156.2; IR (v, KBr, cm^{-1}): 543, 754, 896, 987, 1063, 1106, 1124, 1187, 1266, 1340, 1456; HRMS-ESI (m/z): $[M+H]^+$ Calcd. For ($C_{28}H_{18}F_6NOS$) 530.1008, found: 530.1023.

3.2.4. 1-(1,2-Dimethyl-3-indolyl)-2-[2-methyl-5-(3-quinoline)-3-thienyl]perfluorocyclopentene (3o)

Diarylethene **3o** was prepared by a method similar to that used for **1o**. The crude product was purified by column chromatography on silica gel using petroleum ether and ethyl acetate (v/v = 6/1) as eluent to afford 0.36 g of compound **3o** as a gray solid in 22% yield. Calcd for $C_{29}H_{20}F_6N_2S$ (%): Calcd C, 64.20; H, 3.72; N, 5.12; Found C, 64.21; H, 3.74; N, 5.15; mp: 476–477 K; ^{1}H NMR (400 MHz, $CDCl_3$): δ1.85 (s, 3H), 2.07 (s, 3H), 3.65 (s, 3H), 7.14 (t, 1H, J = 8.0 Hz), 7.23 (t, 1H, J = 8.0 Hz), 7.28 (d, 1H, J = 8.0 Hz), 7.51 (s, 1H), 7.57 (t, 1H, J = 8.0 Hz), 7.60 (d, 1H, J = 8.0 Hz), 7.70 (t, 1H, J = 8.0 Hz), 7.82 (d, 1H, J = 8.0 Hz), 8.09 (d, 1H, J = 8.0 Hz), 8.19 (s, 1H), 9.08 (s, 1H); ^{13}C NMR (100 MHz, $CDCl_3$): δ11.5, 14.8, 30.0, 101.0, 109.2, 116.5, 119.5, 119.6, 119.7, 121.1, 122.1, 124.3, 125.6, 126.8, 127.2, 127.4, 127.7, 127.8, 129.3, 129.5, 131.1, 137.1, 137.9, 138.0, 142.1, 147.3, 148.1; IR (ν, KBr, cm^{-1}): 746, 832, 977, 994, 1045, 1105, 1183, 1272; HRMS-ESI (m/z): $[M+H]^+$ Calcd. For ($C_{29}H_{21}F_6N_2S$) 543.1324, found: 543.1307.

4. Conclusions

In summary, three new asymmetrical diarylethenes with different heteroaryl rings have been synthesized and their structures determined by single-crystal X-ray diffraction analysis. All of them exhibited favorable photochromism and functioned as obvious fluorescence switches in both solution and PMMA films. The results demonstrated that their photochromic behaviors, acidichromism, and fluorescence properties showed dependence on the variable heteroaryl rings. The experimental results provide new evidence for the effects of the heteroaryl moiety and will provide valuable information for the design of new diarylethenes with tunable photochromic properties.

Acknowledgments

This work was supported by the National Natural Science Foundation of China (51373072, 21162011), the Project of Jiangxi Advantage Sci-Tech Innovative Team (20142BCB24012), the Science Funds of Natural Science Foundation of Jiangxi Province (20132BAB203005), and the Project of the Science Funds of Jiangxi Education Office (KJLD12035, GJJ12587, GJJ13577).

References

1. Kawata, S.; Kawata, Y. *Chem. Rev.* **2000**, *100*, 1777–1788.
2. Hou, L. L.; Zhang, X. Y.; Pijper, T. C.; Browne, W. R.; Feringa, B. L. *J. Am. Chem. Soc.* **2014**, *136*, 910–913.
3. Tian, H.; Yang, S. J. *Chem. Soc. Rev.* **2004**, *33*, 85–97.
4. Matsuda, K.; Irie, M. *J. Photoch. Photobio. C* **2004**, *5*, 169–182.
5. Yun, C.; You, J.; Kim, J.; Huh, J.; Kim, E. *J. Photoch. Photobio. C* **2009**, *10*, 111–129.

6. Tsujioka, T.; Irie, M. *J. Photoch. Photobio. C* **2010**, *11*, 1–14.
7. Kudernac, T.; Kobayashi, T.; Uyama, A.; Uchida, K.; Nakamura, S.; Feringa B. L. *J. Phys. Chem. A* **2013**, *117*, 8222–8229.
8. Irie, M. *Chem. Rev.* **2000**, *100*, 1685–1716.
9. Zhang, J. J.; Zou, Q.; Tian, H. *Adv. Mater.* **2013**, *25*, 378–399.
10. Takeshita, M.; Mizukami, E.; Murakami, K.; Wada, Y.; Matsuda, Y. pp. *Eur. J. Org. Chem.* **2014**, *18*, 3784–3787.
11. Higashiguchi, K.; Matsuda, K.; Tanifuji, N.; Irie, M. *J. Am. Chem. Soc.* **2005**, *127*, 8922–8923.
12. Frigoli, M.; Welch, C.; Mehl, G. H. *J. Am. Chem. Soc.* **2004**, *126*, 15382–15383.
13. Moriyama, Y.; Matsuda, K.; Tanifuji, N.; Irie, S.; Irie, M. *Org. Lett.* **2005**, *7*, 3315–3318.
14. Tanifuji, N.; Matsuda, K.; Irie, M. *Org. Lett.* **2005**, *7*, 3777–3780.
15. Zhou, Z. G.; Xiao, S. Z.; Xu, J.; Liu, Z. Q.; Shi, M.; Li, F. Y.; Yi, T.; Huang, C. H. *Org. Lett.* **2006**, *8*, 3911–3914.
16. Jeong, Y. C.; Yang, S. I.; Kim, E.; Ahn, K. H. *Tetrahedron* **2006**, *62*, 5855–5861.
17. Algi, M. P.; Cihaner, A.; Algi, F. *Turk. J. Chem.* **2015**, *39*, 139–148.
18. Gostl, R.; Hecht, S. *Angew. Chem.* **2014**, *126*, 8929–8932.
19. Liu, G.; Pu, S. Z.; Wang, R. J. *Org. Lett.* **2013**, *15*, 980–983.
20. Zheng, C. H.; Pu, S. Z.; Pang Z. Y.; Chen, B.; Liu, G.; Dai, Y. F. *Dyes Pigments* **2013**, *98*, 565–574.
21. Li, X. T.; Pu, S. Z., Li, H.; Liu, G. *Dyes Pigments* **2014**, *105*, 47–56.
22. Yamaguchi, T.; Irie, M. *Tetrahedron Lett.* **2006**, *47*, 1267–1269.
23. Pu, S. Z.; Yang, T. S.; Xu, J. K.; Chen, B. *Tetrahedron Lett.* **2006**, *47*, 6473–6477.
24. Takeshita, M.; Ogawa, M.; Miyata, K.; Yamato, T. *J. Phys. Org. Chem.* **2003**, *16*, 148–151.
25. Yamaguchi, T.; Irie, M. *J. Org. Chem.* **2005**, *70*, 10323–10328.
26. Pu, S. Z.; Wang, R. J.; Liu, G.; Liu, W. J.; Cui, S. Q.; Yan, P. J. *Dyes Pigments* **2012**, *94*, 195–206.
27. Li, Z. X.; Liao, L. Y.; Sun, W.; Xu, C. H.; Zhang, C.; Fang, C. J.; Yan, C. H. *J. Phys. Chem. C.* **2008**, *112*, 5190–5196.
28. Kawai, S.; Nakashima, T.; Atsumi, K.; Sakai, T.; Harigai, M.; Imamoto, Y.; Kamikubo, H.; Kataoka, M.; Kawai, T. *Chem. Mater.* **2007**, *19*, 3479–3483.
29. Higashiguchi, K.; Matsuda, K.; Yamada, T.; Kawai, T.; Irie, M. *Chem. Lett.* **2000**, *29*, 1358–1359.
30. Masakazu, M.; Irie, M. *Chem. Commun.* **2005**, 3895–3905.
31. Morimoto, M.; Irie, M. *Chem. Eur. J.* **2006**, *12*, 4275–4282.
32. Piao, X. J.; Zou, Y.; Wu, J. C.; Li, C. Y.; Yi, T. *Org. Lett.* pp. **2009**, *11*, 3818–3821.
33. Arramel; Pijper, T. C.; Kudernac, T.; Katsonis, N.; van der Maas, M.; Feringa, B. L.; van Wees, B. J. *Nanoscale* **2013**, *5*, 9277–9282.
34. Asadirad, A. M.; Boutault, S.; Erno, Z.; Branda, N. R. *J. Am. Chem. Soc.* **2014**, *136*, 3024–3027.
35. Al-Atar, U.; Fernandes, R.; Johnsen, B.; Baillie, D.; Branda, N. R. *J .Am. Chem. Soc.* **2009**, *131*, 15966–15967.
36. Sun, F. X.; Cui, S. Q.; Liu, G.; Zheng, C. H.; Pu, S. Z. *J. Mol. Struct.* **2015**, *1086*, 131–137.
37. Norsten, T. B.; Branda, N. R. *J .Am. Chem. Soc.* **2001**, *123*, 1784–1785.
38. Chen, B. Z.; Wang, M. Z.; Wu, Y. Q.; Tian, H. *Chem. Commun.* **2002**, 1060–1061.
39. Folling, J.; Polyakova, S.; Belov, V.; Blaaderen, A. V.; Bossi, M. L.; Hell, S. W. *Small* **2008**, *4*, 134–142.
40. Peters, A.; Branda, N. R. *J. Am. Chem. Soc.* **2003**, *125*, 3404–3405.
41. Kim, M. S.; Maruyama, H.; Kawai, T.; Irie, M. *Chem. Mater.* **2003**, *15*, 4539–4543.

42. Logtenberg, H.; van der Velde, J. H. M.; Mendoza, P. d.; Areephong, J.; Hjelm, J.; Feringa, B. L.; Browne, W. R. *J. Phys. Chem. C.* **2012**, *116*, 24136–24142.
43. Kim, Y.; Hellmuth, T. J.; Sysoiev, D.; Pauly, F.; Pietsch, T.; Wolf, J.; Erbe, A.; Huhn, T.; Groth, U.; Steiner, U. E.; et al. *Nano. Lett.* **2012**, *12*, 3736–3742.
44. Algi, M. P.; Cihaner, A.; Algi, F. *Tetrahedron* **2014**, *70*, 5064–5087.
45. Perrier, A.; Maurel, F.; Aubard, J. *J. Photochem. Photobiol. A* **2007**, *189*, 167–176.
46. Tsai, F. C.; Chang, C. C.; Liu, C. L.; Chen, W. C.; Jenekhe, S. A. *Macromolecules* **2005**, *38*, 1958–1966.
47. Zhan, X. W.; Liu, Y. Q.; Wu, X.; Wang, S.; Zhu, D. B. Macromolecules **2002**, *35*, 2529–2537.
48. Liu, G.; Liu, M.; Pu, S. Z.; Fan, C. B.; Cui, S. Q. *Dyes Pigments* **2012**, *95*, 553–562.
49. Ren, P. P.; Wang, R. J.; Pu, S. Z.; Liu, G.; Fan, C. B. *J. Phys. Org. Chem.* **2013**, *27*, 183–190.
50. Pu, S. Z.; Liu, G.; Li, G. Z.; Wang, R. J.; Yang, T. S. *J. Mol. Struct.* **2007**, *833*, 23–29.